3D Magnetic modelling of ellipsoidal bodies

Diego Takahashi Tomazella[1] and Vanderlei C. Oliveira Jr[1]

[1]Department of Geophysics, Observatório Nacional, Rio de Janeiro, Brazil

Correspondence to: Diego Takahashi Tomazella (diego.takahashi@gmail.com)

Abstract.

TEXT

1 Introduction

Based on the mathematical theory of the magnetic induction developed by Poisson (1824), Maxwell (1873) affirmed that, if U is the gravitational potential produced by any body with uniform density ρ and arbitrary shape at a point (x, y, z), then $-\frac{\partial U}{\partial x}$ is the magnetic scalar potential produced at the same point by the same body if it has a uniform magnetization oriented along x with intensity ρ. Maxwell (1873) generalized this idea as a way of determining the magnetic scalar potential produced by any uniformly magnetized body in a given direction. By presuming that this uniform magnetization is due to induction and that it is proportional to the resulting magnetic field (intensity) inside the body, he postulated that the resulting field must also be uniform and parallel to the magnetization. This uniformity is due to the fact that the resulting field is defined as the negative gradient of the magnetic scalar potential. As a consequence of this uniformity, the gravitational potential U at points within the body must be a quadratic function of the spatial coordinates. Apparently, Maxwell (1873) was the first one to postulate that ellipsoids are the only finite bodies having a gravitational potential which satisfies this property and hence can be uniformly magnetized in the presence of a uniform inducing magnetic field. This property can be extended to other bodies defined as limiting cases of an ellipsoid (e.g., spheres, elliptic cylinders), however all the remaining non-ellipsoidal bodies cannot be uniformly magnetized in the presence of a uniform inducing field.

Another particularity of ellipsoids is that they are the only bodies which enable an analytical computation of its self-demagnetization. The self-demagnetization contributes to decrease the magnitude of the magnetization along the shortest axes of a body. It is a function of the body shape and gives rise to shape anisotropy (Uyeda et al., 1963; Thompson and Oldfield, 1986; Dunlop and Özdemir, 1997; Clark and Emerson, 1999; Tauxe, 2003). It is well-established in the literature that the self-demagnetization can be neglected if the body has a susceptibility lower than 0.1 SI (Emerson et al., 1985; Clark et al., 1986; Eskola and Tervo, 1980; Guo et al., 1998, 2001; Purss and Cull, 2005; Hillan and Foss, 2013; Austin et al., 2014; Clark, 2014). However, neglecting the self-demagnetization in geological bodies with high susceptibilities (> 0.1 SI) may strongly mislead the interpretation obtained from magnetic methods. Farrar (1979) demonstrated the importance of the ellipsoidal model in taking into account the self-demagnetization and determining reliable drilling directions on the Tennant Creek field, Australia. Posteriorly, Hoschke (1991) also showed how the ellipsoidal model proved to be highly successful in

locating and defining ironstone bodies in the Tennant Creek field. Clark (2000) provides a good discussion about the influence of the self-demagnetization in magnetic interpretation of the Osborne copper-gold deposit, Australia. This deposit is hosted by ironstone bodies that have very high susceptibility. According to Clark (2000), neglecting the effects of self-demagnetisation led errors of $\approx 55°$ in the interpreted dip. Recently, Austin et al. (2014) used magnetic modelling and rock property measurements to show that, contrary to previous interpretations, the magnetization of the Candelaria iron oxide copper-gold deposit, Chile, is not dominated by the induced component. Rather, the deposit has a relatively weak remanent magnetization and is strongly affected by self-demagnetization. These examples show the importance of the self-demagnetization and the ellipsoidal model in producing trustworthy geological models of high-susceptibility orebodies, which may save significant cost associated with drilling.

A vast literature about the magnetic modelling of ellipsoidal bodies was developed in which are to be found the names of many brilliant researchers. Nevertheless, interest in this subject has not yet died out, as is evidenced by a list of modern papers in this field. Besides, the geoscientific community lacks an easy-to-use tool to simulate the magnetic field produced by uniformly magnetized ellipsoids. Such a tool could prove to be useful either for teaching and researching geophysics. To fill this gap, we provide here a set of routines to model the magnetic field produced by ellipsoids. The routines are written in Python language as part of the Fatiando a Terra (Uieda et al., 2013), which is an open-source library for modelling and inversion in geophysics. We attempt to use the best practices of continuous integration, documentation, unit-testing, and version-control for the purpose of providing a reliable and easy-to-use code. It is hoped that the presentation of the theoretical and practical aspects given here will be found useful to the wide community of geoscientists.

2 Methodology

2.1 Geometrical parameters and coordinate systems

Let (x, y, z) be a point referred to a Cartesian coordinate system with axes x, y and z pointing to, respectively, North, East and down. For convenience, we denominate this coordinate system as *main coordinate system* (Fig. 1a). Let us consider an ellipsoidal body with centre at the point (x_c, y_c, z_c), orientation defined by three angles ε, ζ, and η (Fig. 1a), and semi-axes defined by positive constants a, b, c (Fig. 1b). The angles ε, ζ, and η are called *strike*, *dip*, and *rake*, respectively, and are commonly used to define the orientation of lines in structural geology (Clark et al., 1986; Allmendinger et al., 2012). The points (x, y, z) located on the surface of this ellipsoidal body satisfy the following equation:

$$(\mathbf{r} - \mathbf{r}_c)^T \mathbf{A} (\mathbf{r} - \mathbf{r}_c) = 1 \,, \tag{1}$$

where $\mathbf{r} = [\begin{array}{ccc} x & y & z \end{array}]^\top$, $\mathbf{r}_c = [\begin{array}{ccc} x_c & y_c & z_c \end{array}]^\top$, $\mathbf{A}$ is a positive definite matrix given by

$$\mathbf{A} = \mathbf{V} \begin{bmatrix} a^{-2} & 0 & 0 \\ 0 & b^{-2} & 0 \\ 0 & 0 & c^{-2} \end{bmatrix} \mathbf{V}^\top \,, \tag{2}$$

2

and $\mathbf{V}$ is an orthogonal matrix whose first, second and third columns are defined by unit vectors $\mathbf{v}_1$, $\mathbf{v}_2$, and $\mathbf{v}_3$ (Fig. 1b), respectively. These unit vectors are commonly described in terms of auxiliary orientation angles α, β, and γ, which are not used by the geoscientific community. These angles, however, can be defined from ε, ζ, and η (Fig. 1a) as follows (Clark et al., 1986):

$$5 \quad \alpha = \varepsilon - \cos^{-1}\left[\frac{\cos\eta}{\left(1 - \sin^2\zeta \sin^2\eta\right)^{\frac{1}{2}}}\right], \tag{3}$$

$$\gamma = \tan^{-1}\left(\frac{\cos\zeta}{\sin\zeta \cos\eta}\right) \tag{4}$$

and

$$\delta = \sin^{-1}\left(\sin\zeta \sin\eta\right), \tag{5}$$

10   where $-90° \leq \gamma \leq 90°$ and $0 \leq \delta \leq 90°$. Then, given the orientation angles ε, ζ, and η (Fig. 1a and Eqs. 3, 4, and 5), we define the unit vectors $\mathbf{v}_1$, $\mathbf{v}_2$, and $\mathbf{v}_3$ (Fig. 1b) according to the ellipsoid type. For triaxial ellipsoids (i.e., $a > b > c$), these unit vectors are given by (Clark et al., 1986):

$$\mathbf{v}_1 = \begin{bmatrix} -\cos\alpha \ \cos\delta \\ -\sin\alpha \ \cos\delta \\ -\sin\delta \end{bmatrix}, \tag{6}$$

$$15 \quad \mathbf{v}_2 = \begin{bmatrix} \cos\alpha \ \cos\gamma \ \sin\delta + \sin\alpha \ \sin\gamma \\ \sin\alpha \ \cos\gamma \ \sin\delta - \cos\alpha \ \sin\gamma \\ -\cos\gamma \ \cos\delta \end{bmatrix}, \tag{7}$$

$$\mathbf{v}_3 = \begin{bmatrix} \sin\alpha \ \cos\gamma - \cos\alpha \ \sin\gamma \ \sin\delta \\ -\cos\alpha \ \cos\gamma - \sin\alpha \ \sin\gamma \ \sin\delta \\ \sin\gamma \ \cos\delta \end{bmatrix}. \tag{8}$$

Similarly, the unit vectors $\mathbf{v}_1$, $\mathbf{v}_2$, and $\mathbf{v}_3$ for prolate ellipsoids (i.e., $a > b = c$) are calculated by using Eqs. 6, 7, and 8, but with $\gamma = 0°$ (Emerson et al., 1985). Finally, the unit vectors $\mathbf{v}_1$, $\mathbf{v}_2$, and $\mathbf{v}_3$ for oblate ellipsoids (i.e., $a < b = c$) are calculated
20   as follows:

$$\mathbf{v}_1 = \begin{bmatrix} -\cos\alpha \ \sin\gamma \ \sin\delta + \sin\alpha \ \cos\gamma \\ -\sin\alpha \ \sin\gamma \ \sin\delta - \cos\alpha \ \cos\gamma \\ \sin\gamma \ \cos\delta \end{bmatrix}, \tag{9}$$

$$\mathbf{v}_2 = \begin{bmatrix} -\cos\alpha\,\cos\delta \\ -\sin\alpha\,\cos\delta \\ -\sin\delta \end{bmatrix}, \tag{10}$$

$$\mathbf{v}_3 = \begin{bmatrix} \sin\alpha\,\sin\gamma + \cos\alpha\,\cos\gamma\,\sin\delta \\ -\cos\alpha\,\sin\gamma + \sin\alpha\,\cos\gamma\,\sin\delta \\ -\cos\gamma\,\cos\delta \end{bmatrix}. \tag{11}$$

5 These formulas are similar to those presented by (Emerson et al., 1985).

The magnetic modelling of an ellipsoidal body is commonly performed in a particular Cartesian coordinate system that is aligned with the body semi-axes and has the origin coincident with the body centre (Fig. 1b). For convenience, we denominate this particular coordinate system as *local coordinate system*. The relationship between the Cartesian coordinates $(\tilde{x}, \tilde{y}, \tilde{z})$ of a point in a local coordinate system and the Cartesian coordinates (x, y, z) of the same point in the main system is given by:

10 $\quad \tilde{\mathbf{r}} = \mathbf{V}^\top (\mathbf{r} - \mathbf{r}_c) \,,$ $\tag{12}$

where $\tilde{\mathbf{r}} = \begin{bmatrix} \tilde{x} & \tilde{y} & \tilde{z} \end{bmatrix}^\top$, $\mathbf{r}$ and $\mathbf{r}_c$ are defined in Eq. 1 and the matrix $\mathbf{V}$ (Eq. 2) is defined according to the ellipsoid type. Subsequently, quantities referred to the local coordinate system (Fig. 1b) are represented with the simbol "$\sim$".

2.2   Theoretical background

Consider a magnetized ellipsoid immersed in a uniform inducing magnetic field $\mathbf{H}_0$ (in Am^{-1}) given by

15 $\quad \mathbf{H}_0 = \|\mathbf{H}_0\| \begin{bmatrix} \cos I\,\cos D \\ \cos I\,\sin D \\ \sin I \end{bmatrix}, \tag{13}$

where $\|\cdot\|$ denotes the Euclidean norm (or 2-norm) and D and I are respectively, the declination and inclination of the local-geomagnetic field in the main coordinate system (Fig. 1a). This field represents the main component of the Earth's magnetic field, which is usually assumed to be generated by the Earth's liquid core. In the absence of conduction currents, the total magnetic field $\mathbf{H}(\mathbf{r})$ at the position $\mathbf{r}$ (Eqs. 2 and 12) of a point referred to the main coordinate system is defined as follows

20 (Sharma, 1966; Eskola and Tervo, 1980; Reitz et al., 1992; Stratton, 2007):

$\mathbf{H}(\mathbf{r}) = \mathbf{H}_0 - \nabla V(\mathbf{r}) \,,$ $\tag{14}$

where the second term is the negative gradient of the magnetic scalar potential $V(\mathbf{r})$ given by:

$$V(\mathbf{r}) = -\frac{1}{4\pi} \iiint\limits_{\vartheta} \mathbf{M}(\mathbf{r}')^\top \nabla \left(\frac{1}{\|\mathbf{r} - \mathbf{r}'\|} \right) dx'\,dy'\,dz' \,. \tag{15}$$

4

In this equation, $\mathbf{r}' = [\ x'\ \ y'\ \ z'\ ]^{\top}$ is the position vector of a point located within the volume ϑ, the integral is conducted over the variables x', y' and, z' and $\mathbf{M}(\mathbf{r}')$ is the magnetization vector (in Am^{-1}). Eq. 15 is valid anywhere, independently if the position vector $\mathbf{r}$ represents a point located inside or outside the magnetized body (DuBois, 1896; Reitz et al., 1992; Stratton, 2007).

5   Based on Maxwell's postulate, let us assume that the body has a uniform magnetization given by

$$\mathbf{M} = \mathbf{K}\,\mathbf{H}^{\dagger}\,, \tag{16}$$

where $\mathbf{H}^{\dagger}$ is the resultant uniform magnetic field at any point within the body and $\mathbf{K}$ is a constant and symmetrical 2nd-order tensor representing the magnetic susceptibility of the body. This is a good approximation for bodies at room temperature, subjected to an inducing field $\mathbf{H}_0$ with strength ≤ 1 mT (Rochette et al., 1992). In this case, the susceptibility tensor $\mathbf{K}$ is

10   commonly represented, in the main coordinate system (Fig. 1a), as follows:

$$\mathbf{K} = \mathbf{U} \begin{bmatrix} k_1 & 0 & 0 \\ 0 & k_2 & 0 \\ 0 & 0 & k_3 \end{bmatrix} \mathbf{U}^{\top}\,, \tag{17}$$

where $k_1 > k_2 > k_3$ are the *principal susceptibilities* and $\mathbf{U}$ is an orthogonal matrix whose columns $\mathbf{u}_i$, $i = 1, 2, 3$, are unit vectors called *principal directions*. The unit vectors $\mathbf{u}_i$ may be defined similarly to $\mathbf{v}_1$, $\mathbf{v}_2$, and $\mathbf{v}_3$ (Eqs. 6, 7, 8, 9, 10, and 11), by a given set of orientation angles ε, ζ, and η (Eqs. 3, 4, and 5).

15   If the principal susceptibilities are different from each other, we say that the body has an anisotropy of magnetic susceptibility (AMS). The AMS is generally associated to the preferred orientation of the grains of magnetic minerals forming the rock (Fuller, 1963; Uyeda et al., 1963; Janák, 1972; Hrouda, 1982; Thompson and Oldfield, 1986; MacDonald and Ellwood, 1987; Rochette et al., 1992; Dunlop and Özdemir, 1997; Tauxe, 2003). For the particular case in which the principal directions coincide with the ellipsoid axes, the matrix $\mathbf{U}$ is equal to the matrix $\mathbf{V}$ (Eq. 2). Another important particular case is that in

20   which the susceptibility is isotropic and, consequently, the principal susceptibilities k_1, k_2, and k_3 (Eq. 17) are equal to a constant χ. In this case, the susceptibility tensor $\mathbf{K}$ (Eq. 17) assumes the particular form

$$\mathbf{K} = \chi\,\mathbf{I}\,, \tag{18}$$

where $\mathbf{I}$ represents the identity matrix.

By using the magnetization $\mathbf{M}$ defined by Eq. 16, the total magnetic field $\mathbf{H}(\mathbf{r})$ (Eq. 14) can be rewritten as follows:

25    $$\mathbf{H}(\mathbf{r}) = \mathbf{H}_0 - \mathbf{N}(\mathbf{r})\,\mathbf{K}\,\mathbf{H}^{\dagger}\,, \tag{19}$$

where $\mathbf{N}(\mathbf{r})$ is a symmetrical matrix whose ij-element $n_{ij}(\mathbf{r})$ is given by

$$n_{ij}(\mathbf{r}) = -\frac{1}{4\pi}\frac{\partial^2 f(\mathbf{r})}{\partial r_i\,\partial r_j}\,, \quad i = 1, 2, 3\,, \quad j = 1, 2, 3\,, \tag{20}$$

$r_1 = x$, $r_2 = y$, $r_3 = z$ are the elements of the position vector $\mathbf{r}$ (Eq. 1), and

$$f(\mathbf{r}) = \iiint\limits_{\vartheta} \frac{1}{\|\mathbf{r} - \mathbf{r}'\|}\,dx'dy'dz'\,. \tag{21}$$

Notice that the scalar function $f(\mathbf{r})$ (Eq. 21) is proportional to the gravitational potential that would be produced by the ellipsoidal body with volume ϑ if it had a uniform density equal to the inverse of the gravitational constant. It can be shown that the elements $n_{ij}(\mathbf{r})$ are finite whether $\mathbf{r}$ is a point within or without the volume ϑ (Peirce, 1902; Webster, 1904). The matrix $\mathbf{N}(\mathbf{r})$ (Eq. 19) is called *depolarization tensor* (Solivérez, 1981, 2008).

5   The following part of this paper moves on to describe the magnetic field $\mathbf{H}(\mathbf{r})$ (Eq. 19) at points located both within and without the volume ϑ of the ellipsoidal body. However, the mathematical developments are conveniently performed in the local coordinate system (Fig. 1b) related to the respective ellipsoidal body.

2.3 Coordinate transformation

To continue our description of the magnetic modelling of ellipsoidal bodies, it is convenient to perform two important coordi-

10   nate transformations. The first one transforms the scalar function $f(\mathbf{r})$ (Eq. 21) from the main coordinate system (Fig. 1a) into a new scalar function $\tilde{f}(\tilde{\mathbf{r}})$ referred to the local coordinate system (Fig. 1b). The function $\tilde{f}(\tilde{\mathbf{r}})$ was first presented by Dirichlet (1839) to describe the gravitational potential produced by homogeneous ellipsoids. Posteriorly, several authors also deduced and used this function for describing the magnetic and gravitational fields produced by triaxial, prolate, and oblate ellipsoids (Maxwell, 1873; Thomson and Tait, 1879; DuBois, 1896; Peirce, 1902; Webster, 1904; Kellogg, 1929; Stoner, 1945; Osborn,

15   1945; Peake and Davy, 1953; Macmillan, 1958; Chang, 1961; Lowes, 1974; Clark et al., 1986; Tejedor et al., 1995; Stratton, 2007).

It is convenient to use $\tilde{f}^{\dagger}(\tilde{\mathbf{r}})$ and $\tilde{f}^{\ddagger}(\tilde{\mathbf{r}})$ to define the function $\tilde{f}(\tilde{\mathbf{r}})$ evaluated, respectively, at points $\tilde{\mathbf{r}}$ inside and outside the volume ϑ of the ellipsoidal body. The scalar function $\tilde{f}^{\dagger}(\tilde{\mathbf{r}})$ is given by

$$\tilde{f}^{\dagger}(\tilde{\mathbf{r}}) = \pi\,abc \int\limits_{0}^{\infty} \left(1 - \frac{\tilde{x}^2}{a^2+u} - \frac{\tilde{y}^2}{b^2+u} - \frac{\tilde{z}^2}{c^2+u}\right) \frac{1}{R(u)}\,du\,, \quad \tilde{\mathbf{r}} \in \vartheta\,, \tag{22}$$

20   where

$$R(u) = \sqrt{(a^2+u)\,(b^2+u)\,(c^2+u)}\,. \tag{23}$$

This function represents the gravitational potential that would be produced by the ellipsoidal body at points located within its volume ϑ if it had a uniform density equal to the inverse of the gravitational constant. Notice that, in this case, the gravitational potential is a quadratic function of the spatial coordinates $\tilde{x}$, $\tilde{y}$, and $\tilde{z}$, which supported the Maxwell's (1873) postulate about

25   uniformly magnetized ellipsoids. In a similar way, the function $\tilde{f}^{\ddagger}(\tilde{\mathbf{r}})$ is given by

$$\tilde{f}^{\ddagger}(\tilde{\mathbf{r}}) = \pi\,abc \int\limits_{\lambda}^{\infty} \left(1 - \frac{\tilde{x}^2}{a^2+u} - \frac{\tilde{y}^2}{b^2+u} - \frac{\tilde{z}^2}{c^2+u}\right) \frac{1}{R(u)}\,du\,, \quad \tilde{\mathbf{r}} \notin \vartheta\,, \tag{24}$$

where $R(u)$ is defined by Eq. 23 and the parameter λ is defined according to the ellipsoid type as a function of the spatial coordinates $\tilde{x}$, $\tilde{y}$, and $\tilde{z}$ (see Appendix B). For readers interested in additional information about the parameter λ, we recommend Webster (1904, p. 234), Kellogg (1929, p. 184) and Clark et al. (1986).

The second important coordinate transformation is defined with respect to Eq. 19. By properly using the orthogonality of matrix $\mathbf{V}$ (Eq. 2), the magnetic field $\mathbf{H}(\mathbf{r})$ (Eq. 19) can be transformed from the main coordinate system (Fig. 1a) to the local coordinate system (Fig. 1b) as follows:

$$\underbrace{\mathbf{V}^\top \mathbf{H}(\mathbf{r})}_{\tilde{\mathbf{H}}(\tilde{\mathbf{r}})} = \underbrace{\mathbf{V}^\top \mathbf{H}_0}_{\tilde{\mathbf{H}}_0} - \underbrace{\mathbf{V}^\top \mathbf{N}(\mathbf{r})\mathbf{V}}_{\tilde{\mathbf{N}}(\tilde{\mathbf{r}})} \underbrace{\mathbf{V}^\top \mathbf{K}\mathbf{V}}_{\tilde{\mathbf{K}}} \underbrace{\mathbf{V}^\top \mathbf{H}^\dagger}_{\tilde{\mathbf{H}}^\dagger}, \tag{25}$$

5 where the superscript "~" denotes quantities referred to the respective local coordinate system.

In Eq. 25, the transformed depolarization tensor $\tilde{\mathbf{N}}(\tilde{\mathbf{r}})$ is calculated as a function of the original depolarization tensor $\mathbf{N}(\mathbf{r})$ (Eq. 19). In this case, the elements of $\tilde{\mathbf{N}}(\tilde{\mathbf{r}})$ are calculated as a function of the second derivatives of the function $f(\mathbf{r})$ (Eq. 21), which is defined in the main coordinate system (Fig. 1a). It can be shown (Appendix A), however, that the elements $\tilde{n}_{ij}(\tilde{\mathbf{r}})$ of $\tilde{\mathbf{N}}(\tilde{\mathbf{r}})$ can also be calculated as follows:

10 $$\tilde{n}_{ij}(\tilde{\mathbf{r}}) = -\frac{1}{4\pi}\frac{\partial^2 \tilde{f}(\tilde{\mathbf{r}})}{\partial \tilde{r}_i \partial \tilde{r}_j}, \quad i = 1,2,3, \quad j = 1,2,3, \tag{26}$$

where $\tilde{r}_1 = \tilde{x}$, $\tilde{r}_2 = \tilde{y}$, and $\tilde{r}_3 = \tilde{z}$ are the elements of the transformed vector $\tilde{\mathbf{r}}$ (Eq. 12) and $\tilde{f}(\tilde{\mathbf{r}})$ is given by Eq. 22 or 24, depending if $\tilde{\mathbf{r}}$ represents a point located within or without the volume ϑ of the ellipsoidal body.

2.4 Internal magnetic field and magnetization

By considering $\tilde{\mathbf{r}}$ as a point within the volume ϑ of the ellipsoid and using the Maxwell's postulate about the uniformity of the
15 magnetic field $\mathbf{H}(\mathbf{r})$ inside ellipsoidal bodies, we can use Eq. 25 for defining the resultant uniform magnetic field $\tilde{\mathbf{H}}^\dagger$ inside the ellipsoidal body as follows:

$$\tilde{\mathbf{H}}^\dagger = \left(\mathbf{I} - \tilde{\mathbf{N}}^\dagger \tilde{\mathbf{K}}\right)^{-1} \tilde{\mathbf{H}}_0, \tag{27}$$

where $\mathbf{I}$ is the identity matrix and $\tilde{\mathbf{N}}^\dagger$ is a diagonal matrix representing the transformed depolarization tensor evaluated within the volume ϑ of the ellipsoidal body. For a given ellipsoid, the elements $\tilde{n}_{ii}^\dagger$, $i = 1,2,3$, of $\tilde{\mathbf{N}}^\dagger$ are constants which are expressed
20 in terms of the ellipsoid semi-axes. These elements are presented in detail in a latter section.

Let us pre-multiply the uniform internal field $\tilde{\mathbf{H}}^\dagger$ (Eq. 27) by the transformed susceptibility tensor $\tilde{\mathbf{K}}$ (Eq. 25) to obtain

$$\begin{aligned}\tilde{\mathbf{M}} &= \tilde{\mathbf{K}}\left(\mathbf{I} - \tilde{\mathbf{N}}^\dagger \tilde{\mathbf{K}}\right)^{-1} \tilde{\mathbf{H}}_0 \\ &= \left(\mathbf{I} - \tilde{\mathbf{K}}\tilde{\mathbf{N}}^\dagger\right)^{-1} \tilde{\mathbf{K}}\tilde{\mathbf{H}}_0,\end{aligned} \tag{28}$$

where $\tilde{\mathbf{M}}$ represents the transformed magnetization, as can be easily verified by using Eqs. 16 and 25. The matrix identity used for obtaining the second line of Eq. 28 is given by Searle (1982, p. 151). Equation 28 can be easily generalized for the
25 case in which the ellipsoid has also a uniform remanent magnetization $\tilde{\mathbf{M}}_R$. Let us first consider that the uniform remanent magnetization satisfies the condition $\tilde{\mathbf{H}}_A = \tilde{\mathbf{K}}^{-1}\tilde{\mathbf{M}}_R$, where $\tilde{\mathbf{H}}_A$ represents a hypothetical uniform ancient field. Then, if we assume that $\tilde{\mathbf{H}}_0$, in Eqs. 27 and 28, is in fact the sum of the inducing magnetic field $\tilde{\mathbf{H}}_0$ and the hypothetical ancient field $\tilde{\mathbf{H}}_A$,

we obtain the following generalized equation

$$\mathbf{M} = \mathbf{\Lambda} \left(\mathbf{K}\,\mathbf{H}_0 + \mathbf{M}_R \right), \tag{29}$$

where

$$\mathbf{\Lambda} = \mathbf{V} \left(\mathbf{I} - \tilde{\mathbf{K}}\,\tilde{\mathbf{N}}^\dagger \right)^{-1} \mathbf{V}^\top. \tag{30}$$

5   Despite of the coordinate system transformation represented by the matrix $\mathbf{V}$ (Eq. 2), Eq. 29 is consistent with that given by Clark et al. (1986, Eq. 38). It shows the combined effect of the anisotropy of magnetic susceptibility (AMS) and the shape anisotropy. The AMS is represented by the susceptibility tensor $\mathbf{K}$ (Eq. 17) and reflects the preferred orientation of the magnetic minerals forming the body. The susceptibility tensor appears in Eq. 29, defined in the main coordinate system (Fig. 1a), and Eq. 30, defined in the local coordinate system (Fig. 1b). The shape anisotropy is represented, in Eq.29 by the depolarization

10 tensor $\tilde{\mathbf{N}}^\dagger$ and reflects the self-demagnetization associated to the body shape. Notice that the resultant magnetization $\mathbf{M}$ (Eq. 29) does not necessarily have the same direction as the inducing field $\mathbf{H}_0$ (Eq. 13). The angular difference between the resultant magnetization and the inducing field depends on the combined effect of the anisotropy of magnetic susceptibility and the shape anisotropy.

    For the particular case in which the susceptibility is isotropic, the susceptibility tensor is defined according to Eq. 18. In this

15 case, the magnetization $\mathbf{M}$ (Eqs. 16 and 29), referred to the main coordinate system (Fig. 1a), and the matrix $\mathbf{\Lambda}$ (Eq. 30) can be rewritten as follows:

$$\mathbf{M} = \mathbf{\Lambda} \left(\chi\,\mathbf{H}_0 + \mathbf{M}_R \right), \tag{31}$$

and

$$\mathbf{\Lambda} = \mathbf{V} \left(\mathbf{I} - \chi\,\tilde{\mathbf{N}}^\dagger \right)^{-1} \mathbf{V}^\top. \tag{32}$$

20 Despite the coordinate transformation represented by matrix $\mathbf{V}$ (Eq. 2), this equation is in perfect agreement with those presented by Guo et al. (2001, Eqs. 13–15). The first term, depending on the inducing field $\mathbf{H}_0$ (Eq. 13), represents the induced magnetization whereas the term depending on $\mathbf{M}_R$ is the remanent magnetization. Equation 31 reveals that, as pointed out by many authors (e.g., Maxwell, 1873; DuBois, 1896; Stoner, 1945; Clark et al., 1986; Stratton, 2007), the induced magnetization opposes the inducing field if it is parallel to an ellipsoid axis, independently of the ellipsoid type. Otherwise, the magnetization

25 is not necessarily parallel to the inducing field. If we additionally consider that $\chi << 1$, the matrix $\mathbf{\Lambda}$ (Eq. 32) approaches to the identity and the magnetization $\mathbf{M}$ (Eq. 31) can be approximated by:

$$\breve{\mathbf{M}} = \chi\,\mathbf{H}_0 + \mathbf{M}_R, \tag{33}$$

which is the classical equation describing the resultant magnetization in applied geophysics (Blakely, 1996, p. 89). Notice that, in this particular case, the induced magnetization is parallel to the inducing field $\mathbf{H}_0$ (Eq. 13), whether it is parallel to an

30 ellipsoid axis or not. Usually, Eq. 33 is considered a good approximation for $\chi \leq 0.1$ SI. Although this value has been largely used in the literature, there have been few empirical and/or theoretical investigations about it.

2.4.1 Relationship between χ and the magnetization error

In the case of isotropic susceptibility, the resultant magnetization $\mathbf{M}$ (Eq. 31) may be determined by solving the following linear system:

$$\mathbf{\Lambda}^{-1}\mathbf{M} = \chi\mathbf{H}_0 + \mathbf{M}_R, \tag{34}$$

where, according to Eq. 32,

$$\mathbf{\Lambda}^{-1} = \mathbf{V}\left(\mathbf{I} - \chi\tilde{\mathbf{N}}^{\dagger}\right)\mathbf{V}^{\top}. \tag{35}$$

As we have already pointed out, the approximated magnetization $\breve{\mathbf{M}}$ (Eq. 33) represents the particular case in which the matrix $\mathbf{\Lambda}$ (Eq. 32), and consequently the matrix $\mathbf{\Lambda}^{-1}$ (Eq. 35), are close to the identity. Our goal in this subsection is to bound the norm of the difference between the true magnetization $\mathbf{M}$ (Eqs. 31 and 34) and the approximated magnetization $\breve{\mathbf{M}}$ (Eq. 33). Consider a perturbed matrix $\delta\mathbf{\Lambda}^{-1}$ given by

$$\delta\mathbf{\Lambda}^{-1} = \mathbf{\Lambda}^{-1} - \mathbf{I} \tag{36}$$

and, similarly, a perturbed magnetization vector $\delta\mathbf{M}$ given by

$$\delta\mathbf{M} = \mathbf{M} - \breve{\mathbf{M}}. \tag{37}$$

By using these two equations, we may rewrite that of the approximated magnetization $\breve{\mathbf{M}}$ (Eq. 33) as follows:

$$\left(\mathbf{\Lambda}^{-1} - \delta\mathbf{\Lambda}^{-1}\right)(\mathbf{M} - \delta\mathbf{M}) = \chi\mathbf{H}_0 + \mathbf{M}_R. \tag{38}$$

Now, by subtracting the true magnetization $\mathbf{M}$ (Eq. 34) from this linear system (Eq. 38) and rearranging the terms, we obtain the following linear system for the perturbed magnetization $\delta\mathbf{M}$ (Eq. 37):

$$\delta\mathbf{M} = -\delta\mathbf{\Lambda}^{-1}\mathbf{M}. \tag{39}$$

By using the concept of vector norm and its corresponding operator norm (Demmel, 1997; Golub and Loan, 2013), we may use Eq. 39 to write the following inequality:

$$\frac{\|\delta\mathbf{M}\|}{\|\mathbf{M}\|} \leq \|\delta\mathbf{\Lambda}^{-1}\|. \tag{40}$$

where $\|\delta\mathbf{M}\|$ and $\|\mathbf{M}\|$ denote Euclidean norms (or 2-norms) and the term $\|\delta\mathbf{\Lambda}^{-1}\|$ denotes the matrix 2-norm of $\delta\mathbf{\Lambda}^{-1}$, which is given by

$$\|\delta\mathbf{\Lambda}^{-1}\| = \chi\tilde{n}_{33}^{\dagger}, \tag{41}$$

where $\tilde{n}_{33}^{\dagger}$ is defined in the following sections, depending on the ellipsoid type.

9

2.5 External magnetic field and total-field anomaly

The magnetic field $\Delta\mathbf{H}(\mathbf{r})$ produced by an ellipsoid at external points is calculated from Eqs. 25 and 29 as the difference between the resultant field $\mathbf{H}(\mathbf{r})$ and the inducing field $\mathbf{H}_0$:

$$\Delta\mathbf{H}(\mathbf{r}) = -\mathbf{V}\tilde{\mathbf{N}}^{\ddagger}(\tilde{\mathbf{r}})\,\mathbf{V}^{\top}\mathbf{M}\,. \tag{42}$$

The elements of the transformed depolarization tensor $\tilde{\mathbf{N}}^{\ddagger}(\tilde{\mathbf{r}})$ used in Eq. 42 will be presented in the following section.

The $\Delta\mathbf{H}(\mathbf{r})$ represents the magnetic field produced by a uniformly magnetized body located in the crust. Equation 42 gives the magnetic field (in $\mathrm{A\,m^{-1}}$) produced by an ellipsoid. However, in geophysics, the most widely used field is the magnetic induction (in nT). Fortunately, this conversion can be easily done by multiplying Eq. 42 by $k_m = 10^9\,\mu_0$, where μ_0 represents the magnetic constant (in $\mathrm{H\,m^{-1}}$). For geophysical applications, it is preferable to calculate the total-field anomaly produced by the magnetic sources. This scalar quantity is given by (Blakely, 1996):

$$\Delta T(\mathbf{r}) = \|\mathbf{B}_0 + \Delta\mathbf{B}(\mathbf{r})\| - \|\mathbf{B}_0\|\,, \tag{43}$$

where $\mathbf{B}_0 = k_m\,\mathbf{H}_0$ and $\Delta\mathbf{B}(\mathbf{r}) = k_m\,\Delta\mathbf{H}(\mathbf{r})$, with $\mathbf{H}_0$ and $\Delta\mathbf{H}(\mathbf{r})$ defined, respectively, by Eqs. 13 and 42. In practical situations, however, $\|\mathbf{B}_0\| >> \|\Delta\mathbf{B}(\mathbf{r})\|$ and, consequently, the following approximation is valid (Blakely, 1996):

$$\Delta T(\mathbf{r}) \approx \frac{\mathbf{B}_0^{\top}\Delta\mathbf{B}(\mathbf{r})}{\|\mathbf{B}_0\|}\,. \tag{44}$$

2.6 Transformed depolarization tensors $\tilde{\mathbf{N}}(\tilde{\mathbf{r}})$

2.6.1 Depolarization tensor $\tilde{\mathbf{N}}^{\dagger}$

The elements of the transformed depolarization tensor $\tilde{\mathbf{N}}^{\dagger}$ used in the previous sections are calculated according to Eq. 26, with $\tilde{f}(\tilde{\mathbf{r}})$ given by $\tilde{f}^{\dagger}(\tilde{\mathbf{r}})$ (Eq. 22). As we have already pointed out, the $\tilde{f}^{\dagger}(\tilde{\mathbf{r}})$ (Eq. 22) is a quadratic function of the spatial coordinates $\tilde{x}$, $\tilde{y}$ and $\tilde{z}$. Consequently, the elements $\tilde{n}_{ij}^{\dagger}$, $i = 1,2,3$, $j = 1,2,3$, of $\tilde{\mathbf{N}}^{\dagger}$ do not depend on the elements of the transformed position vector $\tilde{\mathbf{r}}$ (equation 12). Besides, the off-diagonal elements are zero and the diagonal elements are given by (Stoner, 1945):

$$\tilde{n}_{ii}^{\dagger} = \frac{abc}{2}\int\limits_{0}^{\infty}\frac{1}{(e_i^2 + u)\,R(u)}\,du\,, \quad i = 1,2,3\,, \tag{45}$$

where $R(u)$ is defined by Eq. 23 and $e_1 = a$, $e_2 = b$, and $e_3 = c$. These elements are commonly known as *demagnetizing factors* and are defined according to the ellipsoid type. Here, we calculate the demagnetizing factors in the SI system. Consequently, they satisfies the condition $\tilde{n}_{11}^{\dagger} + \tilde{n}_{22}^{\dagger} + \tilde{n}_{33}^{\dagger} = 1$, independently of the ellipsoid type. Notice that, according to Eqs. 25 and A7,

$$\mathbf{N}(\mathbf{r}) = \mathbf{V}\,\tilde{\mathbf{N}}^{\dagger}\,\mathbf{V}^{\top}\,, \tag{46}$$

where $\tilde{\mathbf{N}}^{\dagger}$ is a diagonal matrix and $\mathbf{V}$ (Eq. 2) is an orthogonal matrix. This equation shows that, for the particular case in which $\mathbf{r}$ and consequently $\tilde{\mathbf{r}}$ represent a point inside the volume ϑ of the ellipsoid, the elements $\tilde{n}_{ii}^{\dagger}$ (Eq. 56) of $\tilde{\mathbf{N}}^{\dagger}$ represent the eigenvalues while the columns of $\mathbf{V}$ represent the eigenvectors of the original depolarization tensor $\mathbf{N}(\mathbf{r})$.

Triaxial ellipsoids

For triaxial ellipsoids (e.g., $a > b > c$), the demagnetizing factors obtained by solving Eq. 56 are given by:

$$\tilde{n}_{11}^{\dagger} = \frac{abc}{(a^2 - c^2)^{\frac{1}{2}} (a^2 - b^2)} \left[F(\kappa, \phi) - E(\kappa, \phi) \right] , \tag{47}$$

$$5 \quad \tilde{n}_{22}^{\dagger} = -\frac{abc}{(a^2 - c^2)^{\frac{1}{2}} (a^2 - b^2)} \left[F(\kappa, \phi) - E(\kappa, \phi) \right] + \frac{abc}{(a^2 - c^2)^{\frac{1}{2}} (b^2 - c^2)} E(\kappa, \phi) - \frac{c^2}{b^2 - c^2} \tag{48}$$

and

$$\tilde{n}_{33}^{\dagger} = -\frac{abc}{(a^2 - c^2)^{\frac{1}{2}} (b^2 - c^2)} E(\kappa, \phi) + \frac{b^2}{b^2 - c^2} , \tag{49}$$

where

$$F(\kappa, \phi) = \int_0^{\phi} \frac{1}{\left(1 - \kappa^2 \sin^2 \psi\right)^{\frac{1}{2}}} d\psi , \tag{50}$$

10   and

$$E(\kappa, \phi) = \int_0^{\phi} \left(1 - \kappa^2 \sin^2 \psi\right)^{\frac{1}{2}} d\psi , \tag{51}$$

with $\kappa = \left[\left(a^2 - b^2\right) / \left(a^2 - c^2\right) \right]^{\frac{1}{2}}$ and $\cos \phi = c/a$. The functions $F(\kappa, \phi)$ (Eq. 50) and $E(\kappa, \phi)$ (Eq. 51) are called Legendre's normal elliptic integrals of the first and second kind, respectivelly. Stoner (1945) presented a detailed deduction of the demagnetizing factors $\tilde{n}_{11}^{\dagger}$ (Eq. 47), $\tilde{n}_{22}^{\dagger}$ (Eq. 48) and $\tilde{n}_{33}^{\dagger}$ (Eq. 49). Clark et al. (1986) presented similar formulas. It can be shown

15   that these demagnetizing factors satisfy the conditions $\tilde{n}_{11}^{\dagger} + \tilde{n}_{22}^{\dagger} + \tilde{n}_{33}^{\dagger} = 1$ and $\tilde{n}_{11}^{\dagger} < \tilde{n}_{22}^{\dagger} < \tilde{n}_{33}^{\dagger}$.

Prolate ellipsoids

For prolate ellipsoids (e.g., $a > b = c$), the demagnetizing factors obtained by solving Eq. 56 are given by:

$$\tilde{n}_{11}^{\dagger} = \frac{1}{m^2 - 1} \left\{ \frac{m}{(m^2 - 1)^{\frac{1}{2}}} \ln \left[m + \left(m^2 - 1\right)^{\frac{1}{2}} \right] - 1 \right\} \tag{52}$$

and

$$20 \quad \tilde{n}_{22}^{\dagger} = \frac{1}{2} \left(1 - \tilde{n}_{11}^{\dagger}\right) , \tag{53}$$

where $\tilde{n}_{33}^{\dagger} = \tilde{n}_{22}^{\dagger}$, with $\tilde{n}_{11}^{\dagger}$ defined in Eq. 52 and $m = a/b$. The detailed deduction of the demagnetizing factors $\tilde{n}_{11}^{\dagger}$ (Eq. 52) and $\tilde{n}_{22}^{\dagger}$ (Eq. 53) can be found, for example, in Stoner (1945). These formulas were posteriorly presented by Emerson et al. (1985). It can be shown that these demagnetizing factors satisfy the conditions $\tilde{n}_{11}^{\dagger} + 2\,\tilde{n}_{22}^{\dagger} = 1$ and $\tilde{n}_{11}^{\dagger} < \tilde{n}_{22}^{\dagger}$.

Oblate ellipsoids

For oblate ellipsoids (e.g., $a < b = c$), the demagnetizing factors obtained by solving Eq. 56 are given by:

$$\tilde{n}_{11}^{\dagger} = \frac{1}{1-m^2}\left[1 - \frac{m}{(1-m^2)^{\frac{1}{2}}}\cos^{-1}m\right] \tag{54}$$

and

5 $$\tilde{n}_{22}^{\dagger} = \frac{1}{2}\left(1 - \tilde{n}_{11}^{\dagger}\right), \tag{55}$$

where $\tilde{n}_{33}^{\dagger} = \tilde{n}_{22}^{\dagger}$, with $\tilde{n}_{11}^{\dagger}$ defined in Eq. 54 and $m = a/b$. The detailed deduction of these demagnetizing factors can be found, for example, in Stoner (1945). These formulas can also be found in Emerson et al. (1985). The only difference, however, is that Emerson et al. (1985) replaced the term $\cos^{-1}$ by a term $\tan^{-1}$, according to the trigonometric identity $\tan^{-1} x = \cos^{-1}(1/\sqrt{x^2+1})$, $x > 0$. It can be shown that these demagnetizing factors satisfy the conditions $\tilde{n}_{11}^{\dagger} + 2\,\tilde{n}_{22}^{\dagger} = 1$ and $\tilde{n}_{11}^{\dagger} >$
10 $\tilde{n}_{22}^{\dagger}$.

2.6.2 Depolarization tensor $\tilde{\mathbf{N}}^{\ddagger}(\tilde{\mathbf{r}})$

The elements $\tilde{n}_{ij}^{\ddagger}(\tilde{\mathbf{r}})$, $i = 1, 2, 3$, $j = 1, 2, 3$, of the transformed depolarization tensor $\tilde{\mathbf{N}}^{\ddagger}(\tilde{\mathbf{r}})$ used to compute the magnetic field $\Delta\mathbf{H}(\mathbf{r})$ (Eq. 42) and the total-field anomaly $\Delta T(\mathbf{r})$ (Eqs. 43 and 44) are calculated according to Eq. 26, with $\tilde{f}(\tilde{\mathbf{r}})$ given by $\tilde{f}^{\ddagger}(\tilde{\mathbf{r}})$ (Eq. 24). By following Clark et al. (1986), the diagonal elements $\tilde{n}_{ii}^{\ddagger}$ and the off-diagonal elements $\tilde{n}_{ij}^{\ddagger}$, $i = 1, 2, 3$,
15 $j = 1, 2, 3$, are given by

$$\tilde{n}_{ii}^{\ddagger}(\tilde{\mathbf{r}}) = -\frac{abc}{2}\left(\frac{\partial\lambda}{\partial\tilde{r}_i}h_i\tilde{r}_i + g_i\right) \tag{56}$$

and

$$\tilde{n}_{ij}^{\ddagger}(\tilde{\mathbf{r}}) = -\frac{abc}{2}\left(\frac{\partial\lambda}{\partial\tilde{r}_i}h_j\tilde{r}_j\right), \tag{57}$$

where

20 $$h_i = -\frac{1}{(e_i^2 + \lambda)\,R(\lambda)}, \tag{58}$$

$$g_i = \int_{\lambda}^{\infty}\frac{1}{(e_i^2 + u)\,R(u)}\,du, \tag{59}$$

$e_1 = a$, $e_2 = b$, $e_3 = c$, and $\frac{\partial\lambda}{\partial\tilde{r}_i}$ is defined in Appendix B (Eq. B22). The functions g_i (Eq. 59) are defined according to the ellipsoid type. Notice that the elements $\tilde{n}_{ij}^{\ddagger}$ (Eqs. 56 and 57) are proportional to the second derivatives of the function $\tilde{f}^{\ddagger}(\tilde{\mathbf{r}})$
25 (Eq. 24), which is harmonic. Consequently, the diagonal elements defined in Eq. 56 satisfies the condition $\tilde{n}_{11}^{\ddagger}(\tilde{\mathbf{r}}) + \tilde{n}_{22}^{\ddagger}(\tilde{\mathbf{r}}) + \tilde{n}_{33}^{\ddagger}(\tilde{\mathbf{r}}) = 0$ for any point $\tilde{\mathbf{r}}$ outside the ellipsoid, independently of the ellipsoid type.

Triaxial ellipsoids

For triaxial ellipsoids (e.g., $a > b > c$), the functions g_i (Eq. 59) are defined as follows:

$$g_1 = \frac{2}{(a^2 - b^2)(a^2 - c^2)^{\frac{1}{2}}} \left[F(\kappa, \phi) - E(\kappa, \phi) \right], \tag{60}$$

$$g_2 = \frac{2(a^2 - c^2)^{\frac{1}{2}}}{(a^2 - b^2)(b^2 - c^2)} \left\{ E(\kappa, \phi) - \left(\frac{b^2 - c^2}{a^2 - c^2} \right) F(\kappa, \phi) - \frac{a^2 - b^2}{(a^2 - c^2)^{\frac{1}{2}}} \left[\frac{c^2 + \lambda}{(a^2 + \lambda)(b^2 + \lambda)} \right]^{\frac{1}{2}} \right\} \tag{61}$$

and

$$g_3 = \frac{2}{(b^2 - c^2)(a^2 - c^2)^{\frac{1}{2}}} E(\kappa, \phi) + \frac{2}{b^2 - c^2} \left[\frac{b^2 + \lambda}{(a^2 + \lambda)(c^2 + \lambda)} \right]^{\frac{1}{2}}, \tag{62}$$

where $F(\kappa, \phi)$ and $E(\kappa, \phi)$ are defined by Eqs. 51 and 50, but with $\sin \phi = \sqrt{(a^2 - c^2)/(a^2 + \lambda)}$. A deduction of these formulas was presented by Tejedor et al. (1995). Despite the small differences, these formulas can also be found in Clark et al. (1986).

Prolate ellipsoids

For prolate (e.g., $a > b = c$) ellipsoids, the functions g_i (Eq. 59) are given by:

$$g_1 = \frac{2}{(a^2 - b^2)^{\frac{3}{2}}} \left\{ \ln \left[\frac{(a^2 - b^2)^{\frac{1}{2}} + (a^2 + \lambda)^{\frac{1}{2}}}{(b^2 + \lambda)^{\frac{1}{2}}} \right] - \left(\frac{a^2 - b^2}{a^2 + \lambda} \right)^{\frac{1}{2}} \right\} \tag{63}$$

and

$$g_2 = \frac{1}{(a^2 - b^2)^{\frac{3}{2}}} \left\{ \frac{[(a^2 - b^2)(a^2 + \lambda)]^{\frac{1}{2}}}{b^2 + \lambda} - \ln \left[\frac{(a^2 - b^2)^{\frac{1}{2}} + (a^2 + \lambda)^{\frac{1}{2}}}{(b^2 + \lambda)^{\frac{1}{2}}} \right] \right\}, \tag{64}$$

where $g_3 = g_2$. These formulas can be obtained by properly manipulating those presented by (Emerson et al., 1985).

Oblate ellipsoids

For oblate (e.g., $a < b = c$) ellipsoids, the functions g_i (Eq. 59) are given by:

$$g_1 = \frac{2}{(b^2 - a^2)^{\frac{3}{2}}} \left\{ \left(\frac{b^2 - a^2}{a^2 + \lambda} \right)^{\frac{1}{2}} - \tan^{-1} \left[\left(\frac{b^2 - a^2}{a^2 + \lambda} \right)^{\frac{1}{2}} \right] \right\} \tag{65}$$

and

$$g_2 = \frac{1}{(b^2 - a^2)^{\frac{3}{2}}} \left\{ \tan^{-1} \left[\left(\frac{b^2 - a^2}{a^2 + \lambda} \right)^{\frac{1}{2}} \right] - \frac{[(b^2 - a^2)(a^2 + \lambda)]^{\frac{1}{2}}}{b^2 + \lambda} \right\}, \tag{66}$$

where $g_3 = g_2$. Similarly to the case of prolate ellipsoid shown previously, these formulas can be obtained by properly manipulating those presented by (Emerson et al., 1985).

13

3 Computational implementation and testing

The code is implemented in Python language, by using the NumPy and SciPy libraries (van der Walt et al., 2011), as part of the open-source source library Fatiando a Terra (Uieda et al., 2013). Because of that, it is very modular and has a test suite formed by a considerable number of assertions, unit tests, doc tests and integration tests. For readers interested in automated code testing, we recommend the freely reusable lessons of the Software Carpentry (https://software-carpentry.org/) and at the description of the doctest module available in the documentation for Python 2.X (https://docs.python.org/2/library/doctest.html).

4 Numerical simulations

4.1 Demagnetizing factors

We simulate a triaxial ellipsoid with semi-axes $a_0 = 1000$ m, $b_0 = 700$ m, and $c_0 = 200$ m. Then we use this ellipsoid as a reference to generate 100 different triaxial ellipsoids and calculate their demagnetizing factors $\tilde{n}_{11}^{\dagger}$, $\tilde{n}_{22}^{\dagger}$, and $\tilde{n}_{33}^{\dagger}$ by using Eqs. 47, 48, and 49. The semi-axes of these 100 ellipsoids are given by $a = a_0 + u\,b_0$, $b = b_0 + u\,b_0$, and $c = c_0 + u\,b_0$, where $0 \leq u \leq 10$. Notice that, for $u = 0$, the resulting semi-axes are equal those of the reference ellipsoid. The larger the variable u, the larger the resulting semi-axes a, b, and c, but the smaller the relative difference between them. Consequently, the resulting ellipsoids obtained from the semi-axes a, b, and c become more spherical as u increases. In this case, the demagnetizing factors $\tilde{n}_{11}^{\dagger}$ (Eq. 47), $\tilde{n}_{22}^{\dagger}$ (Eq. 48), and $\tilde{n}_{33}^{\dagger}$ (Eq. 49) tend to $1/3$ (e.g., Stoner, 1945).

Figure 2a shows the calculated demagnetizing factors $\tilde{n}_{11}^{\dagger}$ (in red), $\tilde{n}_{22}^{\dagger}$ (in green), and $\tilde{n}_{33}^{\dagger}$ (in blue) for the 100 triaxial ellipsoids. The result shows that the relative difference between the demagnetizing factors is large for small values of u and decreases as u increases. In this case, all demagnetizing factors tend to $1/3$, according to what we know from theory. Besides, Fig. 2a confirms that the demagnetizing factors satisfy the condition $\tilde{n}_{11}^{\dagger} < \tilde{n}_{22}^{\dagger} < \tilde{n}_{33}^{\dagger}$ independently of the value of u.

We have also simulated 100 different prolate ellipsoids with semi-axes $a = m\,b_0$ and $b = b_0$, where $1.02 \leq m \leq 10$ and $b_0 = 1000$ m, and calculate their demagnetizing factors $\tilde{n}_{11}^{\dagger}$ and $\tilde{n}_{22}^{\dagger}$ by using Eqs. 52 and 53, respectively. Similarly, we simulated 100 different oblate ellipsoids with semi-axes $a = m\,b_0$ and $b = b_0$, where $0.02 \leq m \leq 0.98$ and $b_0 = 1000$ m, and calculate their demagnetizing factors $\tilde{n}_{11}^{\dagger}$ and $\tilde{n}_{22}^{\dagger}$ by using Eqs. 54 and 55, respectively.

Figures 2b and c show the results obtained for the 100 prolate and the 100 oblate ellipsoids, respectively. As expected from theory, the demagnetizing factors $\tilde{n}_{11}^{\dagger}$ (red line in Fig. 2b) and $\tilde{n}_{22}^{\dagger}$ (green line in Fig. 2b) calculated for the prolate ellipsoids are close to $1/3$ for m close to 1. Besides, these demagnetizing factors satisfy the condition $\tilde{n}_{11}^{\dagger} < \tilde{n}_{22}^{\dagger}$ for all values of m. The result obtained for the oblate ellipsoids (Fig. 2c) are also in perfect agreement with theory. The demagnetizing factors $\tilde{n}_{11}^{\dagger}$ (in red) and $\tilde{n}_{22}^{\dagger}$ (in green), which were calculated by using Eqs. 54 and 55, respectively, are close to $1/3$ for m close to 0 and satisfy the condition $\tilde{n}_{11}^{\dagger} > \tilde{n}_{22}^{\dagger}$ for all values of m.

4.2 Susceptibility

TEXT

4.3 Simulation of a geological body

TEXT

5 Conclusions

TEXT

6 Code availability

The code is freely distributed under BSD 3-clause licence as part of the Fatiando a Terra (Uieda et al., 2013), which is an open-source Python library for modelling and inversion in geophysics. Documentation and installation instructions for the most current release version of Fatiando a Terra are provided at http://www.fatiando.org.

Appendix A: Derivatives of the functions $f(\mathbf{r})$ and $\tilde{f}(\tilde{\mathbf{r}})$

Let $\tilde{f}(\tilde{\mathbf{r}})$ be the scalar function obtained by transforming $f(\mathbf{r})$ (Eq. 21) from the main coordinate system (Fig. 1a) to the local coordinate system (Fig. 1b). For convenience, let us rewrite Eq. 12 as follows:

$$\tilde{r}_k = v_{k1}\, r_1 + v_{k2}\, r_2 + v_{k3}\, r_3 + c_k \,, \tag{A1}$$

where $\tilde{r}_k$, $k = 1, 2, 3$, are the elements of the transformed position vector $\tilde{\mathbf{r}}$ (Eq. 12), r_j, $j = 1, 2, 3$, are the elements of the position vector $\mathbf{r}$ (Eq. 1), v_{kj}, $j = 1, 2, 3$, are the elements of the matrix $\mathbf{V}$ (Eq. 2), and c_k is a constant defined by the coordinates x_c, y_c, and z_c of the centre of the ellipsoidal body.

By considering the functions $f(\mathbf{r})$ (Eq. 21) and $\tilde{f}(\tilde{\mathbf{r}})$ evaluated at the same point, but on different coordinate systems, we have:

$$\frac{\partial f(\mathbf{r})}{\partial r_j} = \frac{\partial \tilde{f}(\tilde{\mathbf{r}})}{\partial \tilde{r}_1}\frac{\partial \tilde{r}_1}{\partial r_j} + \frac{\partial \tilde{f}(\tilde{\mathbf{r}})}{\partial \tilde{r}_2}\frac{\partial \tilde{r}_2}{\partial r_j} + \frac{\partial \tilde{f}(\tilde{\mathbf{r}})}{\partial \tilde{r}_3}\frac{\partial \tilde{r}_3}{\partial r_j} \,, \quad j = 1, 2, 3 \,,$$

which, from Eq. A1, can be given by

$$\frac{\partial f(\mathbf{r})}{\partial r_j} = v_{j1}\frac{\partial \tilde{f}(\tilde{\mathbf{r}})}{\partial \tilde{r}_1} + v_{j2}\frac{\partial \tilde{f}(\tilde{\mathbf{r}})}{\partial \tilde{r}_2} + v_{j3}\frac{\partial \tilde{f}(\tilde{\mathbf{r}})}{\partial \tilde{r}_3} \,, \quad j = 1, 2, 3 \,. \tag{A2}$$

Now, by deriving $\frac{\partial f(\mathbf{r})}{\partial r_j}$ (Eq. A2) with respect to the ith element r_i of the position vector $\mathbf{r}$ (Eq. 1), we obtain:

$$\frac{\partial^2 f(\mathbf{r})}{\partial r_i \partial r_j} = v_{j1} \frac{\partial}{\partial r_i}\left(\frac{\partial \tilde{f}(\tilde{\mathbf{r}})}{\partial \tilde{r}_1}\right) + v_{j2}\frac{\partial}{\partial r_i}\left(\frac{\partial \tilde{f}(\tilde{\mathbf{r}})}{\partial \tilde{r}_2}\right) + v_{j3}\frac{\partial}{\partial r_i}\left(\frac{\partial \tilde{f}(\tilde{\mathbf{r}})}{\partial \tilde{r}_3}\right)$$

$$= v_{j1}\left(\frac{\partial^2 \tilde{f}(\tilde{\mathbf{r}})}{\partial \tilde{r}_1 \partial \tilde{r}_1}v_{i1} + \frac{\partial^2 \tilde{f}(\tilde{\mathbf{r}})}{\partial \tilde{r}_2 \partial \tilde{r}_1}v_{i2} + \frac{\partial^2 \tilde{f}(\tilde{\mathbf{r}})}{\partial \tilde{r}_3 \partial \tilde{r}_1}v_{i3}\right) +$$

$$+ v_{j2}\left(\frac{\partial^2 \tilde{f}(\tilde{\mathbf{r}})}{\partial \tilde{r}_1 \partial \tilde{r}_2}v_{i1} + \frac{\partial^2 \tilde{f}(\tilde{\mathbf{r}})}{\partial \tilde{r}_2 \partial \tilde{r}_2}v_{i2} + \frac{\partial^2 \tilde{f}(\tilde{\mathbf{r}})}{\partial \tilde{r}_3 \partial \tilde{r}_2}v_{i3}\right) +$$

$$+ v_{j3}\left(\frac{\partial^2 \tilde{f}(\tilde{\mathbf{r}})}{\partial \tilde{r}_1 \partial \tilde{r}_3}v_{i1} + \frac{\partial^2 \tilde{f}(\tilde{\mathbf{r}})}{\partial \tilde{r}_2 \partial \tilde{r}_3}v_{i2} + \frac{\partial^2 \tilde{f}(\tilde{\mathbf{r}})}{\partial \tilde{r}_3 \partial \tilde{r}_3}v_{i3}\right)$$

$$= \begin{bmatrix} v_{j1} & v_{j2} & v_{j3} \end{bmatrix} \tilde{\mathbf{F}}(\tilde{\mathbf{r}}) \begin{bmatrix} v_{i1} \\ v_{i2} \\ v_{i3} \end{bmatrix} \quad , \tag{A3}$$

where $\tilde{\mathbf{F}}(\tilde{\mathbf{r}})$ is a 3×3 matrix whose ij-th element is $\frac{\partial^2 \tilde{f}(\tilde{\mathbf{r}})}{\partial \tilde{r}_i \partial \tilde{r}_j}$. From Eq. A3, we obtain

$$\mathbf{F}(\mathbf{r}) = \mathbf{V}\tilde{\mathbf{F}}(\tilde{\mathbf{r}})\mathbf{V}^\top , \tag{A4}$$

where $\mathbf{F}(\mathbf{r})$ is a 3×3 matrix whose ij-th element is $\frac{\partial^2 f(\mathbf{r})}{\partial r_i \partial r_j}$ and $\mathbf{V}$ (Eq. 2) is defined according to the ellipsoid type. As one may noticed, the matrices $\mathbf{F}(\mathbf{r})$ and $\tilde{\mathbf{F}}(\tilde{\mathbf{r}})$ represent the Hessians of the functions $f(\mathbf{r})$ (Eq. 21) and $\tilde{f}(\tilde{\mathbf{r}})$, respectively. Besides, the depolarization tensor $\mathbf{N}(\mathbf{r})$ (Eq. 19) can be rewritten by using the matrix $\mathbf{F}(\mathbf{r})$ as follows

$$\mathbf{N}(\mathbf{r}) = -\frac{1}{4\pi}\mathbf{F}(\mathbf{r}) . \tag{A5}$$

By properly using the orthogonality of the matrix $\mathbf{V}$ (Eq. 2), we may rewrite Eq. A4 as follows:

$$\tilde{\mathbf{F}}(\tilde{\mathbf{r}}) = \mathbf{V}^\top \mathbf{F}(\mathbf{r})\mathbf{V} . \tag{A6}$$

Finally, by multiplying both sides of Eq. A6 by $-\frac{1}{4\pi}$ and using Eq. A5, we conclude that

$$\tilde{\mathbf{N}}(\tilde{\mathbf{r}}) = \mathbf{V}^\top \mathbf{N}(\mathbf{r})\mathbf{V} . \tag{A7}$$

Appendix B: Parameter λ and its spatial derivatives

Here, we follow the reasoning presented by Webster (1904) for analysing the parameter λ which defines triaxial, prolate and oblate ellipsoids.

B1 Parameter λ defining triaxial ellipsoids

Let us consider an ellipsoid with semi-axes a, b, c oriented along the $\tilde{x}$-, $\tilde{y}$-, and $\tilde{z}$-axis, respectively, of its local coordinate system (Fig. 1b), where $a > b > c > 0$. This ellipsoid is defined by the following equation:

$$\frac{\tilde{x}^2}{a^2} + \frac{\tilde{y}^2}{b^2} + \frac{\tilde{z}^2}{c^2} = 1 . \tag{B1}$$

A quadric surface (e.g., ellipsoid, hyperboloid of one sheet or hyperboloid of two sheets) which is confocal with the ellipsoid defined in Eq. B1 can be described as follows:

$$\frac{\tilde{x}^2}{a^2 + u} + \frac{\tilde{y}^2}{b^2 + u} + \frac{\tilde{z}^2}{c^2 + u} = 1\,, \tag{B2}$$

where u is a real number. Equation B2 represents an ellipsoid for u satisfying the condition

5   $u + c^2 > 0\,.$ (B3)

Given a, b, c, and a u satisfying B3, we may use B2 for determining a set of points (x, y, z) lying on the surface of an ellipsoid which is confocal with that one defined in Eq. B1. Now, consider the problem of determining the ellipsoid which is confocal with that one defined in B1 and pass through a particular point $(\tilde{x}, \tilde{y}, \tilde{z})$. This problem consists in determining the real number u that, given a, b, c, $\tilde{x}$, $\tilde{y}$, and $\tilde{z}$, satisfies Eq. B2 and the condition expressed by Eq. B3. By rearranging Eq. B2, we

10   obtain the following cubic equation for u:

$$p(u) = (a^2 + u)(b^2 + u)(c^2 + u) - (b^2 + u)(c^2 + u)\tilde{x}^2 - (a^2 + u)(c^2 + u)\tilde{y}^2 - (a^2 + u)(b^2 + u)\tilde{z}^2\,. \tag{B4}$$

This cubic equation shows that:

$$u = \begin{cases} d \to \infty &,\quad p(u) > 0 \\ -c^2 &,\quad p(u) < 0 \\ -b^2 &,\quad p(u) > 0 \\ -a^2 &,\quad p(u) < 0 \end{cases}. \tag{B5}$$

Notice that, according to B5, the smaller, intermediate and largest roots of the cubic equation $p(u)$ (Eq. B4) are located,

15   respectively, in the intervals $[-a^2, -b^2]$, $[-b^2, -c^2]$ and $[-c^2, \infty[$. Remember that we are interested in a u satisfying the condition expressed by Eq. B3. Consequently, according to the signal analysis shown in Eq. B5, we are interested in the largest root λ of the cubic equation $p(u)$ (Eq. B4).

From Eq. B4, we obtain a simpler one given by

$$p(u) = u^3 + p_2\,u^2 + p_1\,u + p_0\,, \tag{B6}$$

20   where

$$p_2 = a^2 + b^2 + c^2 - \tilde{x}^2 - \tilde{y}^2 - \tilde{z}^2\,, \tag{B7}$$

$$p_1 = b^2\,c^2 + a^2\,c^2 + a^2\,b^2 - (b^2 + c^2)\,\tilde{x}^2 - (a^2 + c^2)\,\tilde{y}^2 - (a^2 + b^2)\,\tilde{z}^2 \tag{B8}$$

and

25   $$p_0 = a^2\,b^2\,c^2 - b^2\,c^2\,\tilde{x}^2 - a^2\,c^2\,\tilde{y}^2 - a^2\,b^2\,\tilde{z}^2\,. \tag{B9}$$

Finally, from Eqs. B7, B8 and B9, the largest root λ of $p(u)$ (Eq. B6) can be calculated as follows (Weisstein, 2017):

$$\lambda = 2\sqrt{-Q}\cos\left(\frac{\varphi}{3}\right) - \frac{p_2}{3},$$
(B10)

where

$$\varphi = \cos^{-1}\left(\frac{R}{\sqrt{-Q^3}}\right),$$
(B11)

5

$$Q = \frac{3p_1 - p_2^2}{9}$$
(B12)

and

$$R = \frac{9p_1 p_2 - 27p_0 - 2p_2^3}{54}.$$
(B13)

B2 Parameter λ defining prolate and oblate ellipsoids

10 Let us now consider a prolate ellipsoid with semi-axes a, b, c oriented along the $\tilde{x}$-, $\tilde{y}$-, and $\tilde{z}$-axis, respectively, of its local coordinate system (Fig. 1b), where $a > b = c > 0$. In this case, the Eq. defining the surface of the ellipsoid is obtained by substituting $c = b$ in Eq. B1. Consequently, the equation defining the respective confocal quadric surface is given by

$$\frac{\tilde{x}^2}{a^2 + u} + \frac{\tilde{y}^2 + \tilde{z}^2}{b^2 + u} = 1$$
(B14)

and the new condition that must be fulfilled by the variable u so that Eq. B14 represent an ellipsoid is

15 $u + b^2 > 0$.
(B15)

Similarly to the case of a triaxial ellipsoid presented in the previous subsection, we are interested in determining the real number u that, given a, b, $\tilde{x}$, $\tilde{y}$, and $\tilde{z}$, satisfies Eq. B14 and the condition expressed by Eq. B15. From Eq. B14, we obtain the following quadratic equation for u:

$$p(u) = (a^2 + u)(b^2 + u) - (b^2 + u)\tilde{x}^2 - (a^2 + u)(\tilde{y}^2 + \tilde{z}^2).$$
(B16)

20 This equation shows that

$$u = \begin{cases} d \to \infty & , & f(\rho) > 0 \\ -b^2 & , & f(\rho) < 0 \\ -a^2 & , & f(\rho) > 0 \end{cases}$$
(B17)

and, consequently, that its two roots lie in the intervals $[-a^2, -b^2]$ and $[-b^2, \infty[$. Therefore, according to the condition established by Eq. B15 and the signal analysis shown in Eq. B17, we are interested in the largest root λ of the quadratic equation $p(u)$ (Eq. B16).

18

By properly manipulating Eq. B16, we obtain a simpler one given by

$$p(u) = u^2 + p_1 u + p_0 \,, \tag{B18}$$

where

$$p_1 = a^2 + b^2 - \tilde{x}^2 - \tilde{y}^2 - \tilde{z}^2 \tag{B19}$$

and

$$p_0 = a^2 b^2 - b^2 \tilde{x}^2 - a^2 \left(\tilde{y}^2 + \tilde{z}^2 \right) \,. \tag{B20}$$

Finally, by using Eqs. B19 and B20, the largest root λ of $p(u)$ (Eq. B18) can be easily calculated as follows:

$$\lambda = \frac{-p_1 + \sqrt{p_1^2 - 4 p_0}}{2} \,. \tag{B21}$$

In the case of oblate ellipsoids, the procedure for determining the parameter λ is very similar to this one for prolate ellipsoids. The semi-axes a, b, c of oblate ellipsoids are defined so that $b = c > a > 0$ and the condition that must be fulfilled by the variable u is $u + a^2 > 0$. In this case, the two roots of the resulting quadratic equation lie in the intervals $[-b^2, -a^2]$ and $[-a^2, \infty[$. Consequently, we are still interested in the largest root of the quadratic equation for the variable u, which is also calculated by using Eq. B21.

B3   Spatial derivative of the parameter λ

The magnetic modelling of triaxial, prolate or oblate ellipsoids requires not only the parameter lambda defined by Eqs. B10 and B21, but also its derivatives with respect to the spatial coordinates $\tilde{x}$, $\tilde{y}$, and $\tilde{z}$. Fortunately, the spatial derivatives of the parameter λ can be calculated in a very similar way for all ellipsoid types.

Let us first consider a triaxial ellipsoid. In this case, the spatial derivatives of λ are given by

$$\frac{\partial \lambda}{\partial \tilde{r}_j} = \frac{\frac{2 \tilde{r}_j}{(e_j^2 + \lambda)}}{\left(\frac{\tilde{x}}{a^2 + \lambda} \right)^2 + \left(\frac{\tilde{y}}{b^2 + \lambda} \right)^2 + \left(\frac{\tilde{z}}{c^2 + \lambda} \right)^2} \,, \quad j = 1, 2, 3 \,, \tag{B22}$$

where $\tilde{r}_1 = \tilde{x}$, $\tilde{r}_2 = \tilde{y}$, $\tilde{r}_3 = \tilde{z}$, $e_1 = a$, $e_2 = b$, and $e_3 = c$. This equation can be determined directly from equation B2. The spatial derivatives of λ in the case of prolate or oblate ellipsoids can also be calculated by using Eq. B22 for the particular case in with $b = c$.

References

Allmendinger, R., Cardozo, N., and Fisher, D. M.: Structural geology algorithms : vectors and tensors, Cambridge University Press, 2012.

Austin, J., Geuna, S., Clark, D., and Hillan, D.: Remanence, self-demagnetization and their ramifications for magnetic modelling of iron oxide copper-gold deposits: An example from Candelaria, Chile, Journal of Applied Geophysics, 109, 242 – 255, doi:10.1016/j.jappgeo.2014.08.002, 2014.

Blakely, R. J.: Potential theory in gravity and magnetic applications, Cambridge University Press, 1996.

Chang, H.: Fields external to open-structure magnetic devices represented by ellipsoid or spheroid, British Journal of Applied Physics, 12, 160, 1961.

Clark, D.: Self-Demagnetisation in Practice: the Osborne Cu-Au Deposit, Preview (Magazine of the Australian Society of Exploration Geophysicists), pp. 31–36, 2000.

Clark, D. and Emerson, D.: Self-Demagnetisation, Preview (Magazine of the Australian Society of Exploration Geophysicists), pp. 22–25, 1999.

Clark, D., Saul, S., and Emerson, D.: Magnetic and gravity anomalies of a triaxial ellipsoid, Exploration Geophysics, 17, 189–200, 1986.

Clark, D. A.: Methods for determining remanent and total magnetisations of magnetic sources–a review, Exploration Geophysics, 45, 271–304, 2014.

Demmel, J. W.: Applied Numerical Linear Algebra, SIAM, 1997.

Dirichlet, L. P. G.: Sur un nouvelle methode pour la determination des integrales multiples, Journal de mathématiques pures et appliquées, 1, 164–168, http://sites.mathdoc.fr/JMPA/PDF/JMPA_1839_1_4_A11_0.pdf, 1839.

DuBois, H.: The Magnetic Circuit in Theory and Practice, Longmans, Green, and Co., 1896.

Dunlop, D. and Özdemir, Ö.: Rock Magnetism: Fundamentals and Frontiers, Cambridge Studies in Magnetism, Cambridge University Press, 1997.

Emerson, D. W., Clark, D., and Saul, S.: Magnetic exploration models incorporating remanence, demagnetization and anisotropy: HP 41C handheld computer algorithms, Exploration Geophysics, 16, 1–122, 1985.

Eskola, L. and Tervo, T.: Solving the magnetostatic field problem (a case of high susceptibility) by means of the method of subsections, Geoexploration, 18, 79 – 95, doi:10.1016/0016-7142(80)90022-8, 1980.

Farrar, L.: Some comments on detailed magnetic investigations of ellipsoidal bodies at Tennant Creek, Exploration Geophysics, 10, 26–33, 1979.

Fuller, M. D.: Magnetic anisotropy and paleomagnetism, Journal of Geophysical Research, 68, 293–309, doi:10.1029/JZ068i001p00293, 1963.

Golub, G. H. and Loan, C. F. V.: Matrix Computations (Johns Hopkins Studies in the Mathematical Sciences), Johns Hopkins University Press, 4 edn., 2013.

Guo, W., Dentith, M. C., Li, Z., and Powell, C. M.: Self demagnetisation corrections in magnetic modelling: some examples, Exploration Geophysics, 29, 396–401, 1998.

Guo, W., Dentith, M. C., Bird, R. T., and Clark, D. A.: Systematic error analysis of demagnetization and implications for magnetic interpretation, Geophysics, 66, 562–570, 2001.

Hillan, D. and Foss, C.: Correction schemes for self-demagnetisation, pp. 1–4, doi:10.1071/ASEG2012ab402, 2013.

Hoschke, T.: Geophysical discovery and evaluation of the West Peko copper-gold deposit, Tennant Creek, Exploration Geophysics, 22, 485–495, 1991.

Hrouda, F.: Magnetic anisotropy of rocks and its application in geology and geophysics, Geophysical surveys, 5, 37–82, 1982.

Janák, F.: Magnetic susceptibility anisotropy of various rock types and its significance for geophysics and geology, Geophysical Prospecting, 20, 375–384, doi:10.1111/j.1365-2478.1972.tb00640.x, 1972.

Kellogg, O. D.: Foundations of Potential Theory, Frederick Ungar Publishing Company, 1929.

Lowes, F. J.: The Torque on a Magnet, Proceedings of the Royal Society of London. Series A, Mathematical and Physical Sciences, 337, 555–567, http://www.jstor.org/stable/78532, 1974.

MacDonald, W. D. and Ellwood, B. B.: Anisotropy of magnetic susceptibility: Sedimentological, igneous, and structural-tectonic applications, Reviews of Geophysics, 25, 905–909, doi:10.1029/RG025i005p00905, 1987.

Macmillan, W.: Theory of the Potential, Dover Publications Inc., 1958.

Maxwell, J. C.: A treatise on electricity and magnetism, vol. 2, Clarendon press, 1873.

Osborn, J.: Demagnetizing factors of the general ellipsoid, Physical review, 67, 351, 1945.

Peake, H. J. and Davy, N.: The magnetic fields produced by uniformly magnetized ellipsoids of revolution, British Journal of Applied Physics, 4, 207, 1953.

Peirce, B.: Elements of the Theory of the Newtonian Potential Function, Cornell University Library historical math monographs, Ginn, 1902.

Poisson, S. D.: Second mémoire sur ta théorie du magnétism, Mémoires de l'Académie des sciences de l'Institut de France, pp. 488–533, 1824.

Purss, M. B. J. and Cull, J. P.: A new iterative method for computing the magnetic field at high magnetic susceptibilities, GEOPHYSICS, 70, L53–L62, doi:10.1190/1.2052469, 2005.

Reitz, J. R., Milford, F. J., and Christy, R. W.: Foundations of Electromagnetic Theory, Addison Wesley, 4 edn., 1992.

Rochette, P., Jackson, M., and Aubourg, C.: Rock magnetism and the interpretation of anisotropy of magnetic susceptibility, Reviews of Geophysics, 30, 209–226, doi:10.1029/92RG00733, 1992.

Searle, S. R.: Matrix Algebra Useful for Statistics, Wiley-Interscience, 1982.

Sharma, P. V.: Rapid computation of magnetic anomalies and demagnetization effects caused by bodies of arbitrary shape, pure and applied geophysics, 64, 89–109, doi:10.1007/BF00875535, 1966.

Solivérez, C. E.: Magnetostatics of anisotropic ellipsoidal bodies, IEEE Transactions on Magnetics, 17, 1363–1364, doi:10.1109/TMAG.1981.1061200, 1981.

Solivérez, C. E.: Campos eléctricos generados por elipsoides uniformemente polarizados, Revista mexicana de física E, 54, 203 – 207, 2008.

Stoner, E. C.: The demagnetizing factors for ellipsoids, The London, Edinburgh, and Dublin Philosophical Magazine and Journal of Science, 36, 803–821, 1945.

Stratton, J. A.: Electromagnetic Theory, Wiley-IEEE Press, reissue edn., 2007.

Tauxe, L.: Paleomagnetic principles and practice, Kluwer Academic Publishers, 2003.

Tejedor, M., Rubio, H., Elbaile, L., and Iglesias, R.: External fields created by uniformly magnetized ellipsoids and spheroids, IEEE transactions on magnetics, 31, 830–836, 1995.

Thompson, R. and Oldfield, F.: Environmental Magnetism, Springer Netherlands, 1986.

Thomson, W. and Tait, P.: Treatise on Natural Philosophy, Part II, Cambridge University Press, Cambridge, 1879.

Uieda, L., Oliveira Jr., V. C., and Barbosa, V. C. F.: Modeling the Earth with Fatiando a Terra, in: Proceedings of the 12th Python in Science Conference, edited by van der Walt, S., Millman, J., and Huff, K., pp. 96 – 103, 2013.

Uyeda, S., Fuller, M. D., Belshé, J. C., and Girdler, R. W.: Anisotropy of magnetic susceptibility of rocks and minerals, Journal of Geophysical Research, 68, 279–291, doi:10.1029/JZ068i001p00279, 1963.

5 van der Walt, S., Colbert, S. C., and Varoquaux, G.: The NumPy Array: A Structure for Efficient Numerical Computation, Computing in Science Engineering, 13, 22–30, doi:10.1109/MCSE.2011.37, 2011.

Webster, A.: The Dynamics of Particles and of Rigid, Elastic, and Fluid Bodies: Being Lectures on Mathematical Physics, B. G. Teubners Sammlung von Lehrbüchern auf dem Gebiete der mathematischen Wissenschaften, B.G. Teubner, 1904.

Weisstein, E. W.: Cubic Formula: From MathWorld – A Wolfram Web Resource, http://mathworld.wolfram.com/CubicFormula.html, [On-
10 line; accessed 2017-01-23], 2017.
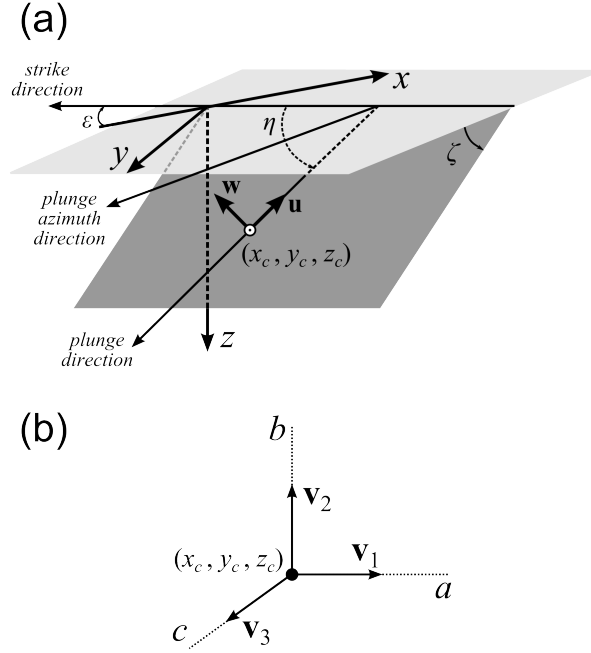
Figure 1. Schematic representation of the coordinate systems used to represent an ellipsoidal body. (a) Main coordinate system with axes x, y, and z pointing to North, East, ans down, respectively. The dark gray plane contains the centre (x_c, y_c, z_c) (white circle) and two unit vectors, $\mathbf{u}$ and $\mathbf{w}$, defining two semi-axes of the ellipsoidal body. For triaxial and prolate ellipsoids, $\mathbf{u}$ and $\mathbf{w}$ define, respectively, the semi-axes a and b. For oblate ellipsoids, $\mathbf{u}$ and $\mathbf{w}$ define the semi-axes b and c, respectively. The strike direction is defined by the intersection of the dark gray plane and the horizontal plane (represented in light gray), which contains the x and y axes. The angle ε between "minus x" and the strike direction is called *strike*. The angle ζ between the horizontal plane and the dark gray plane is called *dip*. The line containing the unit vector $\mathbf{u}$ defines the *plunge direction*. The angle η between the strike direction and the plunge direction is called *rake*. The projection of the plunge direction on the horizontal plane is called *plunge azimuth direction*. (b) Local coordinate system with origin at the ellipsoid centre (x_c, y_c, z_c) (black dot) and axes defined by unit vectors $\mathbf{v}_1$, $\mathbf{v}_2$, and $\mathbf{v}_3$. These unit vectors define the semi-axes a, b, and c of triaxial, prolate, and oblate ellipsoids in the same way. For triaxial and prolate ellipsoids, the unit vectors $\mathbf{u}$ and $\mathbf{w}$ shown in (a) coincide with $\mathbf{v}_1$ and $\mathbf{v}_2$, respectively. For oblate ellipsoids, the unit vectors $\mathbf{u}$ and $\mathbf{w}$ shown in (a) coincide with $\mathbf{v}_2$ and $\mathbf{v}_3$, respectively.
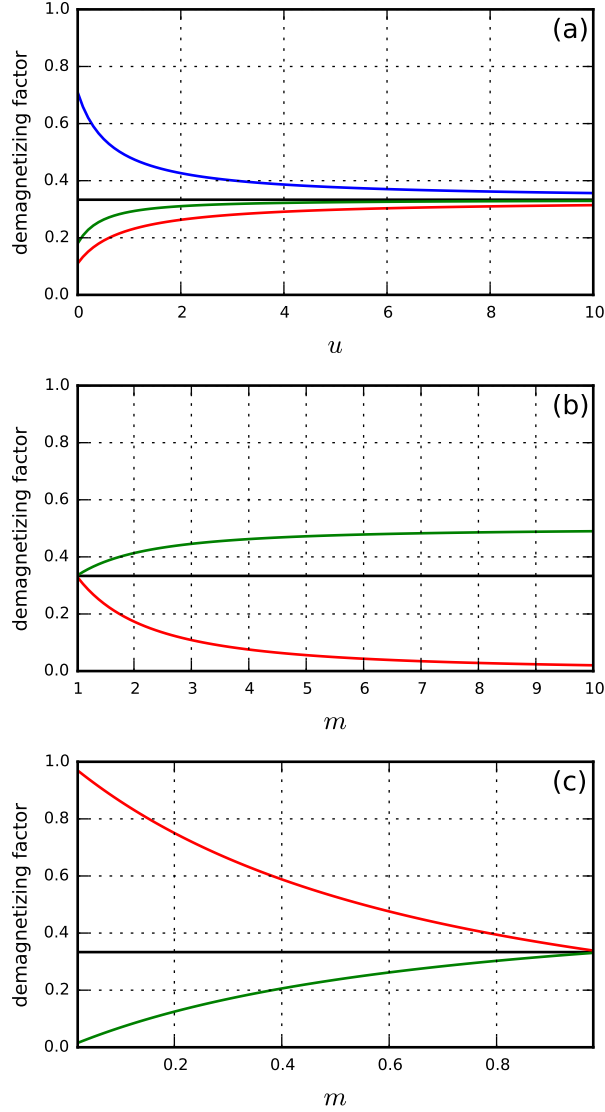
Figure 2. (a) Comparison between the demagnetizing factors $\tilde{n}^{\dagger}_{11}$ (in red), $\tilde{n}^{\dagger}_{22}$ (in green), and $\tilde{n}^{\dagger}_{33}$ (in blue) produced by 100 triaxial ellipsoids with semi-axes $a = a_0 + u\, b_0$, $b = b_0 + u\, b_0$, and $c = c_0 + u\, b_0$, where $0 \leq u \leq 10$ and $b_0 = 700$ m. The demagnetizing factors were calculated by using Eqs. 47, 48, and 49. (b) Comparison between the demagnetizing factors $\tilde{n}^{\dagger}_{11}$ (in red) and $\tilde{n}^{\dagger}_{22}$ (in green) produced by 100 prolate ellipsoids with semi-axes $a = m\, b_0$ and $b = b_0$, where $1.02 \leq m \leq 10$ and $b_0 = 1000$ m. The demagnetizing factors were calculated by using Eqs. 52 and 53. (c) Comparison between the demagnetizing factors $\tilde{n}^{\dagger}_{11}$ (in red) and $\tilde{n}^{\dagger}_{22}$ (in green) produced by 100 oblate ellipsoids with semi-axes $a = m\, b_0$ and $b = b_0$, where $0.02 \leq m \leq 0.98$ and $b_0 = 1000$ m. The demagnetizing factors were calculated by using Eqs. 54 and 55. The horizontal black line represent the value $1/3$.